

PAPER • OPEN ACCESS

Determination Methodology for Stability Domain of Hybrid Electric Power System with Multiple Excitation Sources

To cite this article: Zhongyan Li and Donghai Hu 2019 *IOP Conf. Ser.: Mater. Sci. Eng.* **491** 012020

View the [article online](#) for updates and enhancements.



IOP | ebooks™

Bringing you innovative digital publishing with leading voices to create your essential collection of books in STEM research.

Start exploring the collection - download the first chapter of every title for free.

Determination Methodology for Stability Domain of Hybrid Electric Power System with Multiple Excitation Sources

Zhongyan Li^{1,2} and Donghai Hu^{3,*}

¹School Of Mechanical Engineering, Shanghai Jiao Tong University, Shanghai, 200240, China

²Jinlong United Automotive Industry (Suzhou) Co., Ltd. Suzhou, 215123, China

³School of Automotive and Traffic Engineering, Jiangsu University, Zhenjiang 212013, China

*Corresponding E-mail: 1000004735@ujs.edu.cn

Abstract. Irregular internal excitation (engine excitation and motor excitation) and external load excitation can cause torsional vibration in hybrid electric propulsion system which even leads to the break of shaft. The objective of this paper is to determinate the stability domain of hybrid electric power system under different drive mode with multiple excitation sources. To achieve the goal, the simplified three-mass torsional model of hybrid electric power system is established. Then we apply the multi-scale method to solve the nonlinear torsional model. Finally we set different parameters of engine speed to simulate torsional vibration characteristics of hybrid electric power system. The simulation results exhibit that the torsional vibration characteristics of hybrid electric power system under two drive mode are different because the directional relationship of the moment of engine and permanent magnet synchronous motor (PMSM) is distinctive. It's hard to eliminate the torsional vibration of hybrid electric propulsion system due to phase difference between the engine excitation and the load excitation.

1. Introduction

In recent years, deteriorating energy and environmental problems promote the development of electric power systems and hybrid electric power systems [1,2]. Nevertheless, the application of electric power systems have encountered shortcomings, such as long charging time, limited operating range and lifespan. On the other hand, hybrid electric power systems have been applied increasingly for their flexible working mode, wide operating range and low emission [3,4,5]. Usually, the hybrid electric power system is composed of two power sources: one is the combination of engine and generator, and the other is the combination of motor and battery [6,7]. However, due to the complexity of the configuration of hybrid electric power system and strong nonlinearity of engine and permanent magnet synchronous motor(PMSM), irregular engine excitation and electromagnetic excitation can cause torsional vibration which even leads to the break of shaft [8,9]. So it's essential to analyze the torsional characteristics of hybrid electric power system to determine the stability domain with the engine and PMSM participated in.

The hybrid electric power system is a multi-degree of freedom(DOF) nonlinear system with multiple excitation sources. It is considered that the mass distribution of the hybrid electric power system is lumped [10]. Tang et al. [11] established a 16-DOF torsional vibration model of hybrid



electric vehicle power system. The model is applied to analyze the torsional vibration characteristics and give the theoretical prediction of the natural frequency and corresponding vibration modes. The dynamic model was also used to present the torsional modes of hybrid electric power system in hybrid driving mode. The results indicate that the low frequency vibration is concentrated on the vehicle and wheels. Engine noise is the main noise in the hybrid driving mode. Tang et al. [12] developed a simplified three-mass torsional model of the hybrid electric power system to determine the dominant frequency. The results show that the simplified model can be used to describe the low frequency vibration characteristics of the hybrid electric power system accurately. However, the simplified three-mass model concentrates on the unbalanced torque of engine and does not consider the electromechanical coupling relationship between the engine and motor. Chen et al. [13] established the two-mass torsional vibration model of hybrid electric power system considering electromechanical coupling. Yue et al. [14] specifically analyzed the amplitude-frequency characteristic of torsional vibration in two different modes of the hybrid electric power system (boosting mode and generating mode). The corresponding results of the engine were compared to reveal that the coexistence of electromagnetic torque of motor and the engine torque changes the torsional vibration characteristics of the original engine shafting and intensifies the amplitude of the torsional vibration. Zuo et al. [15] built a multi-body dynamic model based on a simplified structure of a parallel hybrid system. The incentive model of engine was established in MATLAB, the dynamic simulation results show that the change of engine cylinder pressure is the main reason that affects the torsional vibration of the shaft system. However, many researches focus on the influence of engine excitation, as well as the analysis of natural frequencies and corresponding modalities of hybrid electric power system.

The purpose of this paper is to determine the stability domain of hybrid electric power system under two typical drive mode. A simplified three-mass nonlinear torsional model of hybrid electric power system under various drive mode was developed using the lumped parameter method in Section 2. The first-order approximate solution of the model was solved by multi-scale method in Section 3. The nonlinear dynamics theory was applied to reveal the torsional vibration characteristics of hybrid electric power system. Section 4 introduces the results of the influences of variable engine speed on the nonlinear torsional vibration characteristics of hybrid electric power system. Finally, conclusions are drawn in Section 5.

2. Nonlinear torsional model of hybrid electric power system

2.1. Electromagnetic torque model of PMSM

Considering the torsional vibration angle of PMSM, the rotor synthesis fundamental wave magnetomotive force is given below [16,17]:

$$F(\alpha, t) = F_{1m} \cos(\omega t - \alpha) + F_{2m}(\omega t - \alpha + (p\phi + \psi + \pi / 2)) \quad (1)$$

Electromagnetic torque of PMSM is given below when the torsional vibration angel is ϕ .

$$T_M = F_m (\sin \psi \sin(p\phi) - \cos \psi \cos(p\phi)) \quad (2)$$

Where, $F_m = p\pi R l \Lambda_0 F_{1m} F_{2m}$; R is inner radius of stator; l represents effective length of rotor; Λ_0 is air gap permeability of PMSM.

The simplified equation of electromagnetic torque of PMSM is shown using Taylor approximation.

$$T_M = k_0 + k_1\phi - k_2\phi^2 - k_3\phi^3 \quad (3)$$

Where, $k_0 = -F_m \cos \psi$, $k_1 = pF_m \sin \psi$, $k_2 = p^2 F_m / 2 \cos \psi$, $k_3 = p^3 F_m / 6 \sin \psi$.

2.2. Mechanical torque model of engine

The unbalanced force sources of a four-cylinder engine are mainly composed of reciprocating moment of inertia T_j and combustion gas moment T_g . The combustion gas moment T_g can be expressed by

the following infinite series using the Fourier series theory [18,19].

$$T_g = T_0 + \sum_{k=1}^{\infty} c_k \sin(k\alpha + \theta_k) \quad (4)$$

Since the fourth-order and higher-order unbalanced moments are only 2.5% of that of second-order, it is mainly necessary to consider the second-order imbalance torque.

$$\begin{cases} T_j = 2\lambda m_j r^2 \omega^2 \sin 2\alpha \\ T_g = -r\pi D^2 (a_2 \sin 2\alpha + b_2 \cos 2\alpha) / 4 \end{cases} \quad (5)$$

Where, m_j represents reciprocating equivalent mass of piston connecting rod group; r is crank radius; D is piston diameter; λ represents connecting rod ratio.

In actual analysis of engine torsional vibration, only the interference torque T_g generated by changeable gas pressure is generally considered. Furthermore, the cosine component in combustion gas moment T_g is small compared with the sine component. Considering torsional vibration angel, simplified mechanical torque model of engine is given below.

$$T_E = T_0 + \frac{\pi r D^2}{4} a_2 \sin 2\alpha \quad (6)$$

2.3. Nonlinear torsional model under boosting mode

A schematic representation of hybrid electric power system is shown in figure 1. The hybrid electric power system gets into the compound driving mode when the clutch is locked, and the PMSM drives, together with the engine [20,21].

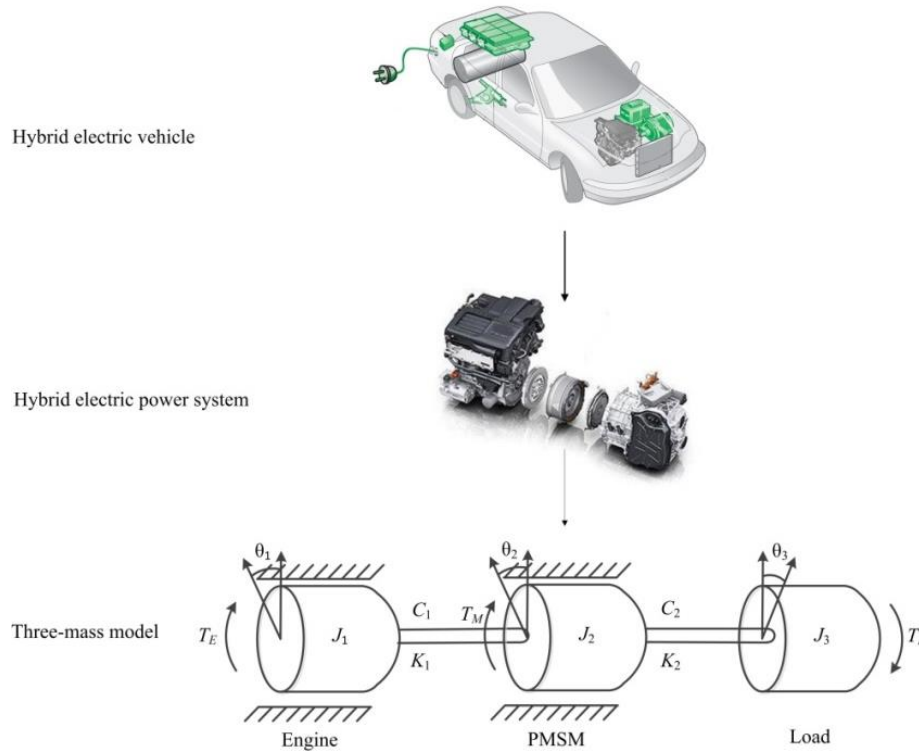


Figure 1. Schema of hybrid electric power system

The mechanical rotation equations is given below:

$$\begin{cases} J_1 \ddot{\theta}_1 + C_1(\dot{\theta}_1 - \dot{\theta}_2) + K_1(\theta_1 - \theta_2) = T_E \\ J_2 \ddot{\theta}_2 + C_1(\dot{\theta}_2 - \dot{\theta}_1) + C_2(\dot{\theta}_2 - \dot{\theta}_3) + K_1(\theta_2 - \theta_1) + K_2(\theta_2 - \theta_3) = T_M \\ J_3 \ddot{\theta}_3 + C_2(\dot{\theta}_3 - \dot{\theta}_2) + K_2(\theta_3 - \theta_2) = -T_L \end{cases} \quad (7)$$

Where J_1 , J_2 and J_3 represent the moment of inertia of engine, PMSM and load respectively; θ_1 , θ_2 , θ_3 represent rotation angles at the end of the two shafts; C_1 and C_2 are damping coefficient; K_1 and K_2 are stiffness of the two shaft respectively.

Suppose that ϕ_{10} , ϕ_{20} and ϕ_{30} are the torsion angles at the ends of the shaft of the hybrid electric propulsion system under the action of constant torques T_{E0} , T_{M0} and T_{L0} respectively. ϕ_1 , ϕ_2 and ϕ_3 are the torsional vibration angles at the end of the shaft under different excitation, respectively. We can get equations shown below:

$$\begin{cases} \theta_1 = \phi_{10} + \phi_1, \theta_2 = \phi_{20} + \phi_2, \theta_3 = \phi_{30} + \phi_3 \\ \dot{\phi}_{10} = \dot{\phi}_{20} = \dot{\phi}_{30} = 0, \ddot{\phi}_{10} = \ddot{\phi}_{20} = \ddot{\phi}_{30} = 0 \end{cases} \quad (8)$$

The equivalent torsional vibration equations of the hybrid electric propulsion system under the engine torque disturbance ΔT_E , electromagnetic torque disturbance term ΔT_M and the load torque disturbance term ΔT_L is given as below:

$$\begin{cases} J_1 \ddot{\phi}_1 + C_1(\dot{\phi}_1 - \dot{\phi}_2) + K_1(\phi_1 - \phi_2) = \Delta T_E \\ J_2 \ddot{\phi}_2 + C_1(\dot{\phi}_2 - \dot{\phi}_1) + C_2(\dot{\phi}_2 - \dot{\phi}_3) + K_1(\phi_2 - \phi_1) + K_2(\phi_2 - \phi_3) = \Delta T_M \\ J_3 \ddot{\phi}_3 + C_2(\dot{\phi}_3 - \dot{\phi}_2) + K_2(\phi_3 - \phi_2) = -\Delta T_L \end{cases} \quad (9)$$

We substitute the following equations into Eqs.9 $\Delta T_E = r\pi D^2 a_2 \sin 2\alpha / 4$, $\Delta T_M = k_1 \phi_2 - k_2 \phi_2^2 - k_3 \phi_2^3$, $\Delta T_L = F \cos(\omega t)$. New variables are set $x_1 = \phi_1 - \phi_2$, $x_2 = \phi_2 - \phi_3$. The nonlinear torsional vibration model of hybrid electric propulsion system is given below:

$$\begin{cases} \ddot{x}_1 + A_1 x_1 + \mu_1 \dot{x}_1 + \mu_3 \dot{x}_2 + (A_2 x_1^2 + B_2 x_2^2 + A_3 x_1^3 + B_3 x_2^3 + D_1 x_1 x_2 + D_2 x_1^2 x_2 + D_3 x_1 x_2^2) = f_1 \sin(\Omega_1 t) \\ \ddot{x}_2 + H_1 x_2 + \mu_4 \dot{x}_1 + \mu_2 \dot{x}_2 - (A_2 x_1^2 + B_2 x_2^2 + A_3 x_1^3 + B_3 x_2^3 + D_1 x_1 x_2 + D_2 x_1^2 x_2 + D_3 x_1 x_2^2) = f_2 \sin(\Omega_2 t) \end{cases} \quad (10)$$

$$\text{Where, } A_1 = \frac{k_1 m_2}{J_2} + \left(\frac{K_1}{J_1} + \frac{K_1}{J_2}\right), A_2 = \frac{k_2 m_2^2}{J_2}, A_3 = -\frac{k_3 m_2^3}{J_2}, B_2 = \frac{k_2 m_1^2}{J_2}, B_3 = \frac{k_3 m_1^3}{J_2}, D_1 = -\frac{2m_1 m_2}{J_2}, \\ D_2 = \frac{3n_3 m_1 m_2^2}{J_2}, D_3 = -\frac{3n_3 m_1^2 m_2}{J_2}, \mu_1 = \frac{C_1}{J_1} + \frac{C_1}{J_2}, H_1 = \frac{K_2}{J_2} + \frac{K_2}{J_3} - \frac{k_1 m_1}{J_2}, \mu_2 = \frac{C_2}{J_2} + \frac{C_2}{J_3}.$$

3. Theoretical analysis of stability domain

First the small parameter ε and the following scale transformation [22] are introduced.

$$\begin{cases} A_i \rightarrow \varepsilon A_i, i = 2, 3; B_i \rightarrow \varepsilon B_i, i = 2, 3; D_i \rightarrow \varepsilon D_i, i = 1, 2, 3 \\ E_1 \rightarrow \varepsilon E_1, G_1 \rightarrow \varepsilon G_1, \mu_i \rightarrow \varepsilon \mu_i, f_i = \varepsilon f_i, i = 1, 2 \end{cases} \quad (11)$$

The two-degree-of-freedom nonlinear model with the combination of parameter excitation and external excitation is shown as follows.

$$\begin{cases} \ddot{x}_1 + \omega_1^2 x_1 + \varepsilon(A_2 x_1^2 + B_2 x_2^2 + A_3 x_1^3 + B_3 x_2^3 + D_1 x_1 x_2 + D_2 x_1^2 x_2 + D_3 x_1 x_2^2 + \mu_1 \dot{x}_1 + \mu_3 \dot{x}_2) = \varepsilon f_1 \sin(\Omega_1 t) \\ \ddot{x}_2 + \omega_2^2 x_2 - \varepsilon(A_2 x_1^2 + B_2 x_2^2 + A_3 x_1^3 + B_3 x_2^3 + D_1 x_1 x_2 + D_2 x_1^2 x_2 + D_3 x_1 x_2^2 - \mu_4 \dot{x}_1 - \mu_2 \dot{x}_2) = \varepsilon f_2 \sin(\Omega_2 t) \end{cases} \quad (12)$$

We use the method of multiple scales to find the first-order uniform asymptotic solution of Eqs. 12.

$$\begin{cases} \omega_1(t, \varepsilon) = x_{10}(T_0, T_1) + \varepsilon x_{11}(T_0, T_1) \\ \omega_2(t, \varepsilon) = x_{20}(T_0, T_1) + \varepsilon x_{21}(T_0, T_1) \end{cases} \quad (13)$$

Where, $T_0 = t, T_1 = \varepsilon t$.

We introduce two tuning parameters σ_1 and σ_2 .

$$\omega_1^2 = \Omega^2 + \varepsilon^2 \sigma_1, \omega_2^2 = \Omega^2 + \varepsilon^2 \sigma_2 \quad (14)$$

Eqs. 13 and 14 are substituted into Eqs. 12 to make the coefficients of the same power of ε on both sides of the equation equal.

ε^0 :

$$\begin{cases} D_0^2 x_{10} + \omega_1^2 x_{10} = 0 \\ D_0^2 x_{20} + \omega_2^2 x_{20} = 0 \end{cases} \quad (15)$$

ε^1 :

$$\begin{cases} D_0^2 x_{11} + \Omega^2 x_{11} = -2D_0 D_1 x_{10} - (A_2 x_{10}^2 + B_2 x_{20}^2 + A_3 x_{10}^3 + B_3 x_{20}^3 + D_1 x_{10} x_{20} + D_2 x_{10}^2 x_{20} + D_3 x_{10} x_{20}^2) \\ -\mu_1 \dot{x}_{10} - \mu_3 \dot{x}_{20} + f_1 \sin(\Omega_1 t) \\ D_0^2 x_{21} + \Omega^2 x_{21} = -2D_0 D_1 x_{20} + (A_2 x_{10}^2 + B_2 x_{20}^2 + A_3 x_{10}^3 + B_3 x_{20}^3 + D_1 x_{10} x_{20} + D_2 x_{10}^2 x_{20} + D_3 x_{10} x_{20}^2) \\ -\mu_4 \dot{x}_{10} - \mu_2 \dot{x}_{20} + f_2 \sin(\Omega_2 t) \end{cases} \quad (16)$$

The solution of the complex form of Equation 15 can be expressed as follows:

$$\begin{cases} x_{10} = A(T_1, T_2) e^{i\omega_1 T_0} + CC \\ x_{20} = B(T_1, T_2) e^{i\omega_2 T_0} + CC \end{cases} \quad (17)$$

Where CC represents the complex conjugate.

The elimination conditions for secular term is shown below.

$$\begin{cases} -2D_1 A \Omega_1 - 3A_3 A^2 \bar{A} - 3B_3 B^2 \bar{B} - D_2 \bar{A}^2 B - D_3 \bar{A} B^2 - \mu_1 A \Omega - \mu_3 B \Omega = 0 \\ -2D_1 B \Omega_1 - 3A_3 A^2 \bar{A} - 3B_3 B^2 \bar{B} - D_2 \bar{A}^2 B - D_3 \bar{A} B^2 - \mu_2 B \Omega - \mu_4 A \Omega = 0 \end{cases} \quad (18)$$

We let $A = (x_1 + iy_1)/2, B = (x_2 + iy_2)/2$ and bring to Eqs. 18 and separate the real imaginary part to get the following average equations.

$$\begin{cases} x_1' = 0.5\mu_1 x_1 + 0.5\mu_3 x_2 + Na_1 \\ y_1' = -0.5\mu_1 y_1 - 0.5\mu_3 y_2 + Na_2 \\ x_2' = 0.5\mu_4 x_1 + 0.5\mu_2 x_2 + Na_3 \\ y_2' = 0.5\mu_4 y_1 - 0.5\mu_2 y_2 + Na_4 \end{cases} \quad (19)$$

Where, $Na_i, i=1,2,3,4$ is nonlinear functions and the symbol $'$ represents the derivative of the slow time scale T_1 .

The characteristic equation at the zero solution has the following form:

$$\lambda^4 + R_1 \lambda^3 + R_2 \lambda^2 + R_3 \lambda + R_4 = 0 \quad (20)$$

According to the Routh-Hurwitz principle [23], the stability conditions is given as follows.

$$\begin{cases} R_1 > 0 \\ R_1 R_2 - R_3 > 0 \\ R_3(R_1 R_2 - R_3) - R_1^2 R_4 > 0 \\ R_4 > 0 \end{cases} \quad (21)$$

4. Numerical simulation results of stability domain

4.1. Under boosting mode

Time history diagram and phase portraits of x_1 obtained by simulation when $\omega_1=150, \omega_1=200, \omega_1=250$ are shown in figure 2. The initial values are set to be $x_{10}=x_{20}=\dot{x}_{10}=\dot{x}_{20}=0$, and the load excitation frequency is set to be $\omega_2=20$.

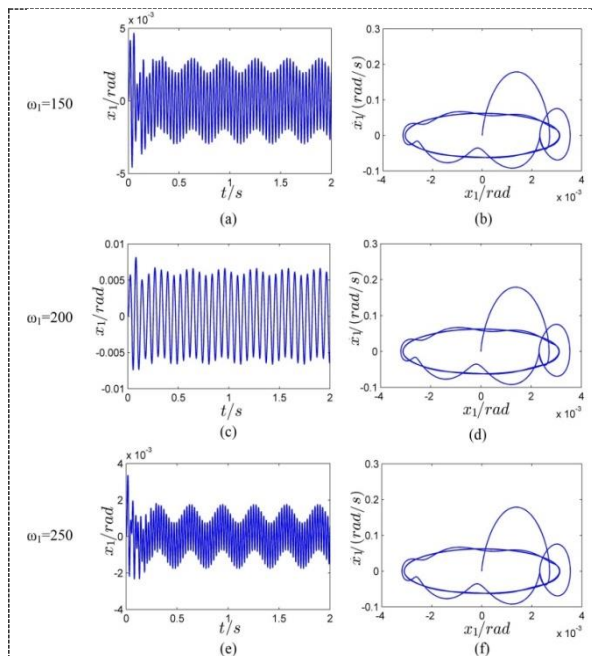


Figure 2. Time history and phase portraits of x_1 with different engine speed

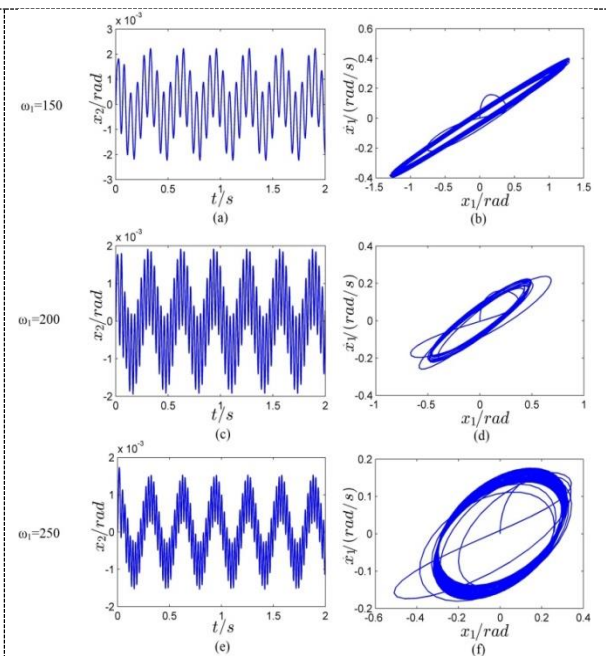


Figure 3. Time history and phase portraits of x_2 with different engine speed.

The Poincaré bifurcation diagram of x_1 with variation of parameter the rotational speed of engine ω_1 is shown in figure 4. When $150 < \omega_1 < 200$, the torsional vibration of shaft between engine and PMSM gets gradually stable, while the torsional vibration of the shaft gradually loses stability with increasing engine speed when $200 < \omega_1 < 250$.

Time history diagram and phase portraits of x_2 obtained by simulation when $\omega_1=150, \omega_1=200$ are shown in figure 3. The initial values are set to be $x_{10}=x_{20}=\dot{x}_{10}=\dot{x}_{20}=0$, and the load excitation frequency is set to be $\omega_2=20$. The Poincaré bifurcation diagram of x_2 with variation of parameter the rotational speed of engine ω_1 is shown in figure 5.

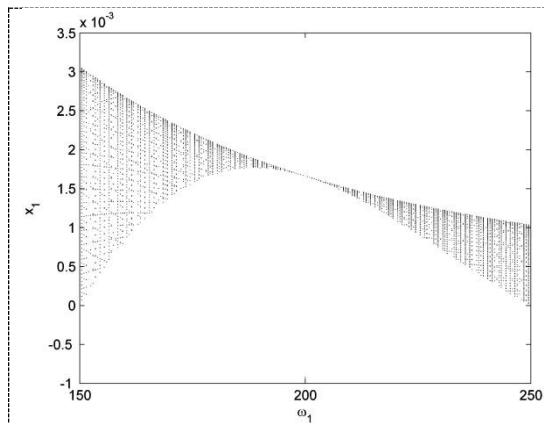


Figure 4. The Poincaré bifurcation diagram of x_1 with variation of parameter the rotational speed of engine ω_1

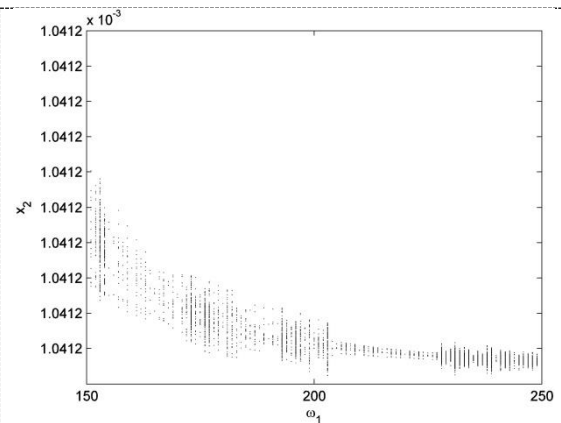


Figure 5. The Poincaré bifurcation diagram of x_2 with variation of parameter the rotational speed of engine ω_1

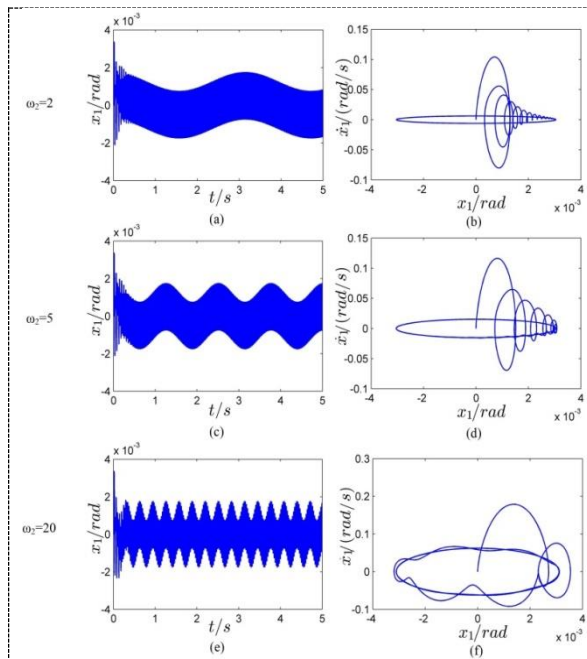


Figure 6. The Poincaré bifurcation diagram of x_1 with variation of load excitation frequency.

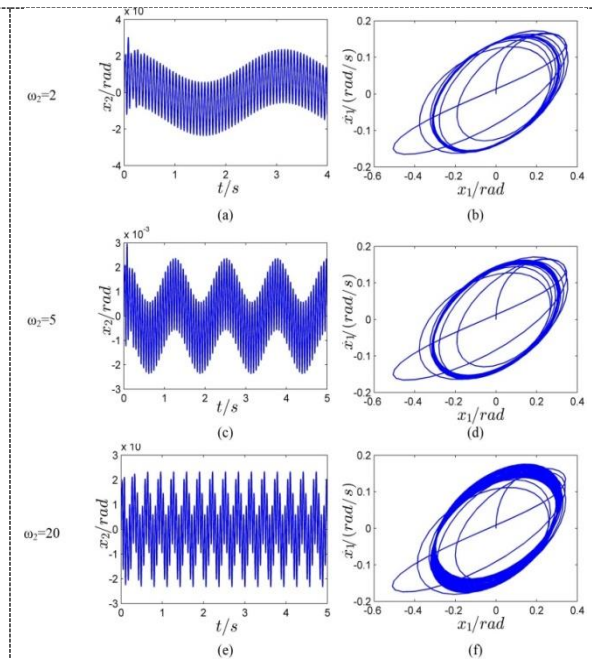


Figure 7. Time history and phase portraits of x_2 with different load excitation frequency.

4.2. Under generating mode

Time history diagram and phase portraits of x_1 obtained by simulation are shown in figure 6. The initial values are set to be $x_{10}=x_{20}=\dot{x}_{10}=\dot{x}_{20}=0$, and the engine speed is set to be $\omega_1=200$. The Poincaré bifurcation diagram of x_1 with variation of load excitation frequency ω_2 is shown in figure 8.

Time history diagram and phase portraits of x_2 obtained by simulation when $\omega_2=2, \omega_2=5, \omega_2=20$, are shown in figure 7. The initial values are set to be $x_{10}=x_{20}=\dot{x}_{10}=\dot{x}_{20}=0$, and the load excitation frequency is set to be $\omega_1=200$. The Poincaré bifurcation diagram of x_2 with variation of load excitation frequency ω_2 is shown in figure 9.

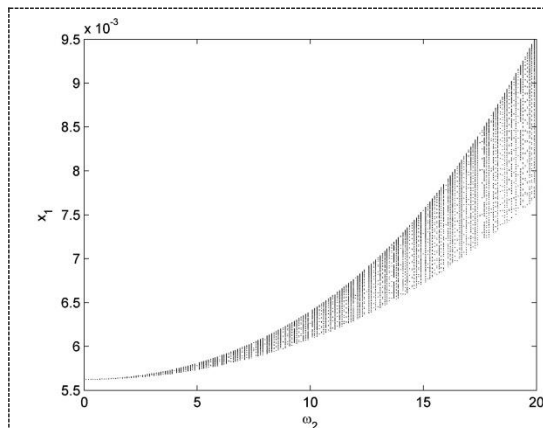


Figure 8. The Poincaré bifurcation diagram of x_1 with variation of load excitation frequency ω_2 .

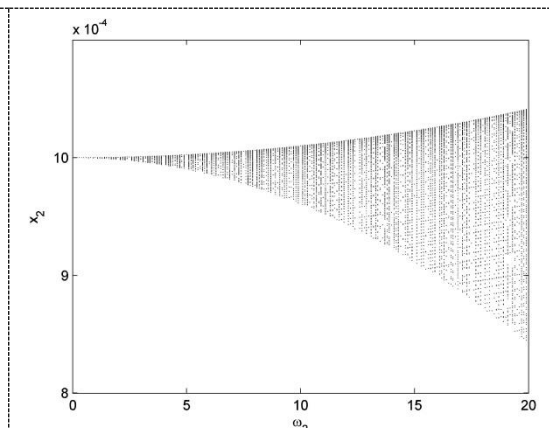


Figure 9. The Poincaré bifurcation diagram of x_2 with variation of load excitation frequency of engine ω_2 .

5. Conclusion

In this paper, a three-mass torsional vibration model of engine-PMSM-load of hybrid electric propulsion system is established by using lumped parameter method. Using nonlinear dynamics theory, the influence of different engine speed and load excitation frequency on nonlinear torsional vibration stability of hybrid electric propulsion system is studied. We get the following conclusions:

(1) There is a phase difference between the engine excitation and the load excitation in the hybrid electric propulsion system, which makes the hybrid electric propulsion system hard to eliminate the torsional vibration;

(2) With the engine speed as the control parameter, the torsional vibration characteristics of the two shaft are different because the directional relationship of the moment of engine and PMSM is distinctive from that of PMSM and load. When $150 < \omega_1 < 200$, the torsional vibration of shaft between engine and PMSM gets gradually stable, while the torsional vibration of the shaft gradually loses stability with increasing engine speed when $200 < \omega_1 < 250$.

(3) With the load excitation frequency as the control parameter, as the load excitation frequency increases, the torsional vibration of the hybrid electric propulsion system gradually loses stability.

Funding

This work was supported by the National Natural Science Foundation of China (grant no. 51275291), National Natural Science Foundation of China (grant no. 51705208) and China Postdoctoral Science Foundation (grant no. 2018M632240).

References

- [1] Liang L, Wang X, and Song J 2016 *MECH SYST SIGNAL PR* **87** 17-29.
- [2] Chan C.C 2007 *PROC IEEE* **95** 704-718.
- [3] Chao Y, Song J, Li L and Cao D 2016 *MECH SYST SIGNAL PR* **77** 649-664.
- [4] Bradley T H, and Frank A A 2009 *Renew. Sust. Energ. Rev* **13** 115-128.
- [5] Inman S, El-Gindy M, Haworth D C 2003 *INT J HEAVY VEH SYST* **10** 167-187.
- [6] Yang Y, Hu X, Pei H and Peng Z 2016 *Appl. Energy* **168** 683-690.
- [7] JonasFredriksson, HenrikWeiefors and BoEgardt 2002 *Veh. Syst. Dyn* **37** 359-376.
- [8] Guo X and He H 2016 *MATEC Web of Conferences* **81** p08002.
- [9] Abouobaia E, Bhat R and Sedaghati R 2015 *J INTEL MAT SYST STR* **1** 1-13.
- [10] Ebrahimi M, Farshidianfar A and Bartlett H 2003 *Proc. Inst. Mech. Eng. Part D-J* **215** 217-229.
- [11] Tang X, Jin Y, Zhang J, Zou L and Yu H 2014 *Proc. Inst. Mech. Eng. Part D-J* **228** 94-103.

- [12] Tang X, Yang W, Hu X and Zhang D 2017 *MECH SYST SIGNAL PR* **85** 329-338.
- [13] Chen K, Hu J and Peng Z 2017 *Energy Procedia* **105** 3164-3172.
- [14] Yue D, Miao D and Zhang J 2008 *Auto. Eng* **3** 211-214.
- [15] Zuo J, Liu S, Huang Z and Hu Q 2012 *Appl. Mech. Mat* **190** 825-831
- [16] Yu Y and Mi Z 2013 *J Appl. Math* 1-11.
- [17] Chen X, Yuan S and Peng Z 2015 *Nonlinear Dyn* **80** 541-552.
- [18] Burston, Amanda, Ward B and Davies R 2001 *MON NOT R ASTRON SOC* **326** 403-415.
- [19] Ying G, Meng G and Jing J 2009 *Arch. Appl. Mech* **79** 287-299.
- [20] Chen L, Xi G and Sun J 2012 *IEEE T VEH TECHNOL* **61** 2936-2949.
- [21] Du C and Ding X 2015 *IAEAC* 905-910.
- [22] Cacan, Martin R, Stephen L and Leamy M 2014 *Nonlinear Dyn* **78** 1205-1220.
- [23] Cermak, J and Nechvatal L 2017 *Nonlinear Dyn* **87** 939-954.